Biomedicine & Pharmacotherapy 161 (2023) 114461

Contents lists available at ScienceDirect

Biomedicine & Pharmacotherapy

journal homepage: www.elsevier.com/locate/biopha

Diosmin mitigates dexamethasone-induced osteoporosis in vivo: Role of Runx2, RANKL/OPG, and oxidative stress

El-Shaimaa A. Arafa [a,b,c,*,1], Noran O. Elgendy [c,d,1], Mai A. Elhemely [e,c,1], Eglal A. Abdelaleem [f,1], Wafaa R. Mohamed [c,**,1]

[a] College of Pharmacy and Health Sciences, Ajman University, Ajman 346, United Arab Emirates
[b] Center of Medical and Bio-Allied Health Sciences Research, Ajman University, Ajman 346, United Arab Emirates
[c] Department of Pharmacology and Toxicology, Faculty of Pharmacy, Beni-Suef University, Beni-Suef 62514, Egypt
[d] Department of Clinical Pharmacy, Beni-Suef University Hospital, Faculty of Medicine, Beni-Suef University, Beni-Suef, Egypt
[e] School of Medical Sciences, Faculty of Biology, Medicine and Health, The University of Manchester, Manchester M20 4GJ, United Kingdom
[f] Department of Pharmaceutical Analytical Chemistry, Faculty of Pharmacy, Beni-Suef University, Beni-Suef 62514, Egypt

ARTICLE INFO

Keywords:
Osteoporosis
Glucocorticoids
Diosmin
RANKL/OPG
Runx-2
Oxidative stress

ABSTRACT

Secondary osteoporosis is commonly caused by long-term intake of glucocorticoids (GCs), such as dexamethasone (DEX). Diosmin, a natural substance with potent antioxidant and anti-inflammatory properties, is clinically used for treating some vascular disorders. The current work targeted exploring the protective properties of diosmin to counteract DEX-induced osteoporosis in vivo. Rats were administered DEX (7 mg/kg) once weekly for 5 weeks, and in the second week, vehicle or diosmin (50 or 100 mg/kg/day) for the next four weeks. Femur bone tissues were collected and processed for histological and biochemical examinations. The study findings showed that diosmin alleviated the histological bone impairments caused by DEX. In addition, diosmin upregulated the expression of Runt-related transcription factor 2 (Runx2) and phosphorylated protein kinase B (*p*-AKT) and the mRNA transcripts of Wingless (Wnt) and osteocalcin. Furthermore, diosmin counteracted the rise in the mRNA levels of receptor activator of nuclear factor-kB ligand (RANKL) and the reduction in osteoprotegerin (OPG), both were induced by DEX. Diosmin restored the oxidant/antioxidant equilibrium and exerted significant anti-apoptotic activity. The aforementioned effects were more pronounced at the dose level of 100 mg/kg. Collectively, diosmin has proven to protect rats against DEX-induced osteoporosis by augmenting osteoblast and bone development while hindering osteoclast and bone resorption. Our findings could be used as a stand for recommending supplementation of diosmin for patients chronically using GCs.

1. Introduction

Osteoporosis is a condition of diminished bone density and altered structure, leading to high risk of fractures [1]. The reduction in bone mass occurs when osteoclast-moderated bone resorption exceeds osteoblast-moderated bone development. Osteoporosis affects about 200 million people worldwide [2], and it remains asymptomatic until a fracture occurs [3]. It is broadly divided into two types: primary and secondary [4]. Primary osteoporosis can occur as a result of the natural aging process and after menopause. Osteoporosis can be secondary to medical conditions, such as rheumatoid arthritis and endocrine disorders, or chronic use of medications, including glucocorticoids (GCs) and hormonal therapy [5]. GCs, such as dexamethasone (DEX), are widely used in the management of numerous inflammatory and autoimmune conditions and post-transplant operations. However, long-term administration of GCs induces osteoporosis, which is considered the most common form of secondary osteoporosis. It has been reported that about 30–50 % of patients receiving GCs on a chronic basis develop fractures [6].

The pathogenesis of GCs-induced osteoporosis is mediated mainly through effects on osteoblasts, osteocytes and osteoclasts [7]. GCs suppress osteoblastogenesis by downregulating Runt-related transcription

* Corresponding author at: College of Pharmacy and Health Sciences, Ajman University, Ajman 346, United Arab Emirates.
** Corresponding author.
E-mail addresses: e.arafa@ajman.ac.ae (E.-S.A. Arafa), wafaa.mohamed@pharm.bsu.edu.eg (W.R. Mohamed).
[1] All authors contributed equally.

https://doi.org/10.1016/j.biopha.2023.114461
Received 5 December 2022; Received in revised form 31 January 2023; Accepted 26 February 2023
Available online 6 March 2023

factor-2 (Runx2) which fosters osteoblast differentiation and maturation into osteocytes, thereby supporting bone formation [8,9]. In addition, GCs stimulate apoptosis of osteoblasts and osteocytes, causing a reduced rate of bone development and bone loss [10,11]. Another important signaling pathway facilitating osteoblast differentiation is that of Wingless (Wnt) which is also disrupted by the excessive use of GCs [7]. It has been revealed that the canonical Wnt/β-catenin signalling pathway boosts osteoblastogenesis and bone development [12] while repressing osteoclast activity [13]. Interestingly, Runx2 and Wnt reciprocally regulate their expression [14]. Equally, GCs suppress the production of osteocalcin from the differentiated osteoblasts [15]. Osteocalcin, the most copious noncollagenous protein present in bone, is required for bone mineralization since it binds calcium and hydroxyapatite, making a strong bone matrix [16]. A small amount of osteocalcin is normally released into circulation acting as a hormone to regulate insulin secretion and function [17,18]. However, a high serum level of osteocalcin is detected in conditions of excessive bone degradation such as osteoporosis [19].

Protein kinase B (known as Akt) is involved in crucial cell survival paths, including the phosphatidylinositol 3-kinase (PI3K)/Akt pathway. Phosphoactivation of the PI3K/Akt pathway has been revealed to stimulate osteoblast proliferation, differentiation and bone formation along with antagonizing apoptosis, thereby mitigating osteoporosis [20]. In turn, downregulating the PI3K/Akt pathway has shown to contribute to GCs-induced bone impairment in vitro and in vivo [21].

Furthermore, GCs enhance RANKL/OPG axis-mediated osteoclastogenesis via upregulation of receptor activator of nuclear factor-kB ligand (RANKL), which is a proosteoclastic cytokine, and downregulation of osteoprotegerin (OPG) which is an antiosteoclastic cytokine [8,22]. Oxidative stress significantly participates in the pathogenesis of osteoporosis as well as other diseases [23]. Oxidative stress precipitates from elevated generation of reactive oxygen species (ROS) coupled with reduced body ability to eliminate them, hence tissue damage may occur. DEX has been reported to generate a high level of ROS with subsequent induction of osteoblast apoptosis, osteoclastogenesis and bone loss [24].

Current treatments of osteoporosis, such as bisphosphonates, are associated with serious adverse effects, including jaw osteonecrosis and renal toxicity [25]. In turn, it is important to find more effective and safe alternatives for managing osteoporosis. Diosmin (diosmetin-7-O-rutinoside) is a natural flavone diglycoside abundantly found in the pericarp of many citrus fruits. Its structure and biochemical properties are closely related to another flavonoid compound called hesperidin [26,27]. Diosmin is mostly subject to rapid intestinal hydrolysis into diosmetin, which is then absorbed into the circulation and well distributed into tissues [28,29]. Diosmin has been revealed to possess antioxidant, anti-inflammatory, antihyperlipidemic, and anti-hyperglycaemic features [30–33]. Additionally, several in vivo studies have demonstrated its antifibrotic, anticancer, neuroprotective and nephroprotective effects [26]. It is worthy to mention that diosmin is available in a pharmaceutical preparation called Daflon® (90 % diosmin and 10 % hesperidin) and is prescribed for the management of varicose veins, hemorrhoids and lymphedema [26].

Since diosmin is safe for human use, researchers are encouraged to experimentally validate its efficacy against other diseases, including osteoporosis. To this end, the antiosteoporotic effect of diosmin has been previously investigated. For instance, Sharma et al. [34] and Hu et al. [35] showed that diosmin could protect rats from bone loss induced by chronic kidney disease and ovariectomy, respectively. Besides, a composition containing diosmin and hesperidin demonstrated the ability to enhance bone regeneration in a rat femur osteotomy model [29]. Yet, the skeletal and molecular effects of diosmin were not elucidated against GCs-induced osteoporosis. Accordingly, we aimed to explore the potential antiosteoporotic effect of diosmin against DEX-instigated osteoporosis and to identify its molecular mechanisms, particularly the role of Runx2, Wnt, Akt pathway, RANKL/OPG system, and oxidative stress.

2. Material and Methods

2.1. Materials and Animals

Diosmin was obtained from Sedico Pharmaceutical company, Egypt. Epidron® (EIPICO, Egypt), an injection containing DEX sodium phosphate 4 mg/ml, was used as our source of DEX.

Male Wistar rats (200–250 g) obtained from Nahda University (Beni-Suef, Egypt) were used in the present study. Animal care, handling and procedures were performed following the Research Ethics Committee of Faculty of Pharmacy, Beni-Suef University (REC-A-PhBSU-20004). Animals were housed as six per cage and maintained at 25 °C and 12–12 h cycles with ad libitum food and water.

2.2. Experimental design

Animals were allocated into five groups (n = 8), namely control, DIO 100, DEX, DEX+DIO 50 and DEX+DIO 100. All groups except the 1st and 2nd groups received a weekly intramuscular injection of 7 mg/kg DEX for five weeks. DEX+DIO 50 and DEX+DIO 100 groups received 50 mg/kg/day and 100 mg/kg/day diosmin respectively, orally for four weeks starting from the 2nd week of DEX administration. The control group was intramuscularly injected with isotonic saline once a week for five weeks and orally received vehicle (1 % carboxymethyl cellulose) daily for the last four weeks. In addition to having an intramuscular injection of isotonic saline, once a week for five weeks, DIO 100 group received diosmin 100 mg/kg/day orally for four weeks. The given doses of DEX and diosmin were selected based on published work [34,36].

Animals were sacrificed by end of the 5th week. Femur bones were separated and washed. Left femur bones were kept at −80 °C for further analysis, while right ones were fixed in formol saline for histopathological assessment.

2.3. Histopathological analyses

Bone samples were fixed for 48 hrs in 10 % buffered formalin solution, decalcified for 20 days using Cal-X II (Thermo-Fisher Scientific), processed with serial dilutions of ethanol, cleared in xylene and implanted in Paraplast tissue medium. Sections of 5 μm thick were cut, and stained with hematoxylin and eosin (H&E) for histological examination of tissue samples or Masson's Goldner Trichrome staining (Sigma-Aldrich) for the differentiation of mineralized and non-mineralized areas in the bone matrix [37]. Six non-overlapping fields were arbitrarily picked and investigated from every H & E stained bone section for the determination of mean trabecular bone area, mean trabecular bone width, and mean cortical bone width. Fields selected from Masson's Goldner trichrome-stained sections were utilized to determine the relative area percentage of the non-mineralized bone matrix known as osteoid. Histopathological examination was performed using microscopic imaging system (Leica Microsystems GmbH, Germany).

2.4. Enzyme-linked immunosorbent assay (ELISA)

The protein expression of Runx2, anti-apoptotic B-cell lymphoma 2 (BCL2) and pro-apoptotic BCL2-associated X protein (BAX) in rat bone tissues were quantified using ELISA kits: Aviva Systems Biology (Cat# OKEH05960), BioVision (Cat# E4513–100) and LifeSpan BioSciences (Cat# LS-F4135), respectively. The assays were conducted per manufacturer's recommendations.

2.5. Western blot analysis

Proteins were extracted from femur bone tissues utilizing Tris lysis buffer/protease inhibitor cocktail (Biospes, China) and the total protein concentration was determined according to Bradford method [38].

Samples (50 μg total protein) were separated by gel electrophoresis and transferred to PVDF membranes [39]. Membranes were incubated with the primaryantibodies against Akt, *p*-Akt, and β-actin (Santa Cruz, Dallas, USA; dilution 1:1000). Following three washes, incubation of membranes for 1 h with the secondary antibody was done (Santa Cruz, Dallas, USA, 1:5000 dilution in TBST). The BCIP/NBT substrate detection Kit was used to visualize the bands (Genemed Biotechnologies, San Francisco, USA), followed by band assessment utilizing image J® (National Institutes of Health, Bethesda, USA) relative to β-actin, the internal control of protein loading.

2.6. Real-time quantitative polymerase chain reaction (RT-qPCR)

Total RNA was extracted from rat bone tissue using GF-1 Total RNA extraction kit (Vivantis Technologies, Malaysia). SPECTROstar Nano spectrometer (BMG Labtech, France) was used for assessing RNA concentration. 2-steps RT-PCR kit (Vivantis Technologies, Malaysia) was used for cDNA synthesis and performing SYBR green RT-PCR, per manufacturer's instructions. Table 1. contains all the primers used (Vivantis Technologies, Malaysia). The obtained data were then utilized to determine the fold change of gene expression relative to the normal control group using the $2^{-\triangle\triangle Ct}$ [40]. GAPDH was used as the endogenous reference gene.

2.7. Assessment of oxidative stress markers

Homogenate of slices taken from femur bone tissue was used to estimate alterations in the bone oxidative/antioxidative status. To determine the antioxidative status of bone, glutathione (GSH) and superoxide dismutase (SOD) contents were measured utilizing ELISA kits (GSH: Eagle Biosciences, Cat# GLU39-K01; SOD: Cusabio, Cat# CSB-EL022397RA). Lipid peroxidation, the oxidative stress biomarker, was assessed by measuring malondialdehyde (MDA) content colorimetrically in bone tissue using a kit (Eagle Biosciences, Cat# LIP39-K01).

2.8. Statistical analysis

Statistical analysis was carried out using GraphPad Prism version 5.0 (San Diego, CA). Data passed Shapiro-Wilk normality test and were presented as mean ± SEM One-way analysis of variance (ANOVA) followed by Tukey-Kramer multiple comparisons test was utilized to calculate the significance level of differences among groups. $P < 0.05$ was used as the level of significance.

3. Results

3.1. Diosmin alleviates DEX-induced bone histopathological changes

Sections taken from the control and DIO 100 groups demonstrated normal histological architectures of meshwork structure of bony trabeculae (yellow star) and normally distributed osteoblasts and osteocytes with normal widening of intertrabecular spaces (blue star) without abnormal alteration of bone marrow cellularity (Fig. 1**A**). It also showed intact intercellular mineralized bony matrix (Masson's Goldner Trichrome stain, Fig. 2**A**) andnormally organized osseous tissue structures in cortical bones with minimal cracks or porosity records (Fig. 3).

Sections from DEX-treated rats showed deformity and disorganization of bone elements including a significant reduction of the percentage of trabecular bone areas and trabecular bone's width (yellow star; Fig. 1**A**, **B**) relative to control. In addition, severe loss of bone marrow cellular elements and replacement with adipose tissue, which was accompanied by obvious vacuolation (blue star, Fig. 1**A**, **B**). Moreover, it showed a significant increase in the area percentage of osteoid (non-mineralized bone matrix; Fig. 2**A, B**) as well as a significant decrease in cortical bone thickness (Fig. 3).

Sections from DEX+DIO 50 group showed a significant decline in the percentage of trabecular bone area, mean trabecular bone width (yellow star, Fig. 1**A, B**) and mean cortical bone width (Fig. 3) compared to control. In addition, mild persistent bone marrow hypoplasia and adipose tissue hyperplasia (blue star, Fig. 1**A**) is present. However, there was a marked decrease in the percentage of non-mineralized bone matrix area in Masson's Goldner Trichrome-stained sections (Fig. 2**A, B**).

Sections from DEX+DIO 100 group showed a significant improvement in the percentage of trabecular bone areas and mean trabecular bone width (yellow star, Fig. 1**A**, **B**) compared to DEX group. Moreover, restoration of bone marrow cellular components (blue star, Fig. 1**A**) was observed. The effects exerted by DIO 100 were significant compared with DEX+DIO 50 group which suggests the dose-dependent effect of DIO. DEX+DIO 100 showed a significant rise in cortical bone width in comparison to DEX group and DEX+DIO 50 (Fig. 3). In Masson's Goldner Trichrome-stained sections, there was a marked decrease in the percentage of non-mineralized bone matrix area (Fig. 2**A, B**) compared to DEX group.

3.2. Diosmin elevates Runx2 protein expression suppressed by DEX

Administration of DEX for five weeks significantly reduced Runx2 protein expression in femur tissues by 62.6 % compared to control group. However, DEX+DIO 50 and DEX+DIO 100 groups demonstrated a significant increase in Runx2 level to 1.6-fold and 2.2-fold, respectively, in comparison to the DEX-treated rats. Moreover, normalization of Runx2 level was observed in DEX+DIO 100 group. Interestingly, Runx2 level was markedly higher in DEX+DIO 100 group than that of DEX+DIO 50, indicating a dose-dependent effect of diosmin. It is worth mentioning that treatment with 100 mg/kg/day diosmin for four weeks didn't significantly alter the normal level of Runx2 protein (Fig. 4).

3.3. Diosmin augments Wnt and osteocalcin mRNA expression reduced by DEX

The qRT-PCR analysis of femoral bone tissues of DEX group demonstrated downregulated mRNA expression levels of Wnt and osteocalcin relative to control group. In contrast, the expression levels of Wnt and osteocalcin were substantially increased in DEX+DIO 100 group to 10.7 fold ($P < 0.05$) and 4.9 fold ($P < 0.01$), respectively, in comparison to DEX group (Fig. 5).

3.4. Diosmin promotes Akt phosphorylation reduced by DEX

The expression level of *p*-Akt, the active, phosphorylated form of Akt, was significantly curbed in the femur tissue of DEX group by 79.5 % ($P < 0.001$) relative to control group, while Akt level remained unchanged. Subsequently, *p*-Akt/Akt ratio was reduced by 78.4 % ($P < 0.001$). On the other hand, administration of 100 mg/kg diosmin combined with DEX increased *p*-Akt/Akt ratio to 3.3-fold ($P < 0.05$) in comparison to DEX group, indicating enhanced phosphorylation of Akt (Fig. 6).

Table 1
Primer sequences of the studied genes.

Targeted genes	Sequence
RANKL	**F:** ACCAGCATCAAAATCCCAAG **R:** TTTGAAAGCCCCAAAGTACG
OPG	**F:** GTTCTTGCACAGCTTCACCA **R:** AAACAGCCCAGTGACCATTC
Wnt	**F:** TTTAGCCCGAGCAGGAAAGG **R:** TCTACCACAGATGGCGAGGA
Osteocalcin	**F:** CTAGCGGACCACATTGGCTT **R:** GCTGTGCCGTCCATACTTTC
GAPDH	**F:** TGCTGGTGCTGAGTATGTCG **R:** TTGAGAGCAATGCCAGCC

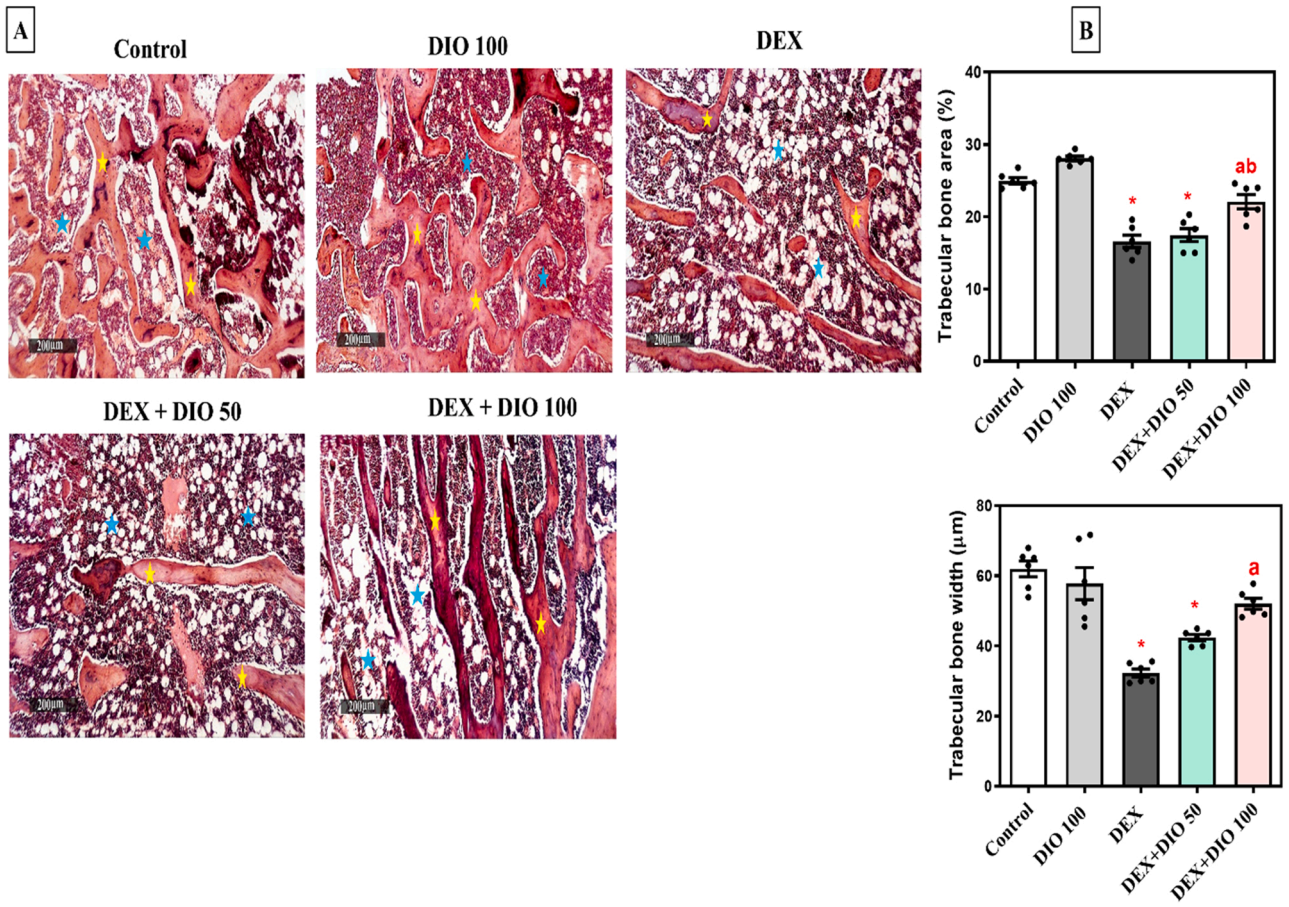

Fig. 1. Effect of diosmin on DEX-induced histopathological changes in rat femur tissue. A) photomicrographs of H & E-stained sections of femur tissues (yellow stars, trabecular bone; blue stars, bone marrow). Magnification = 100x, Scale bar = 200 µm. B) Morphometric analysis of trabeculae showing trabecular bone area and width. * significant difference from control; [a] significant difference from DEX; [b] significant difference from DEX+DIO 50. DEX, dexamethasone; DIO, diosmin.

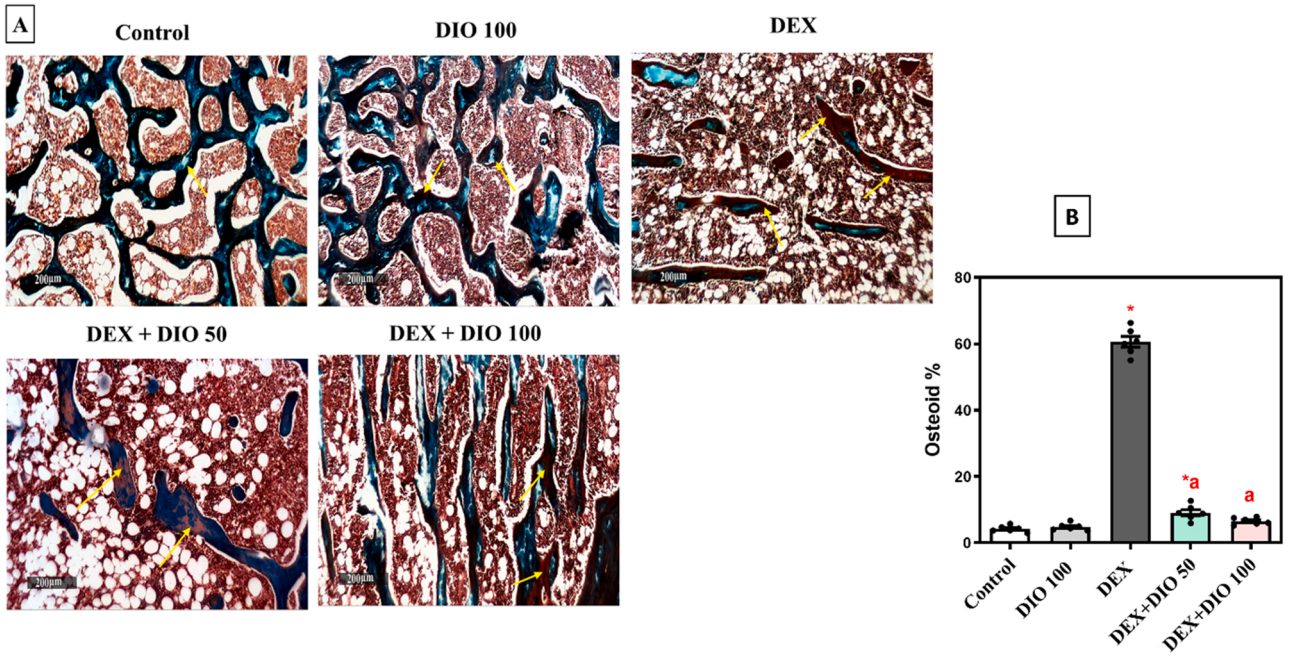

Fig. 2. Effect of diosmin on non-mineralized bone matrix area percentage (osteoid). A) photomicrographs of Masson's Goldner-stained sections of femur tissues (yellow arrow, mineralized bony matrix). Magnification = 100x, scale bar = 200 µm. B) Morphometric analysis of osteoid percentage. * significant difference from control; [a] significant difference from DEX. DEX, dexamethasone; DIO, diosmin.

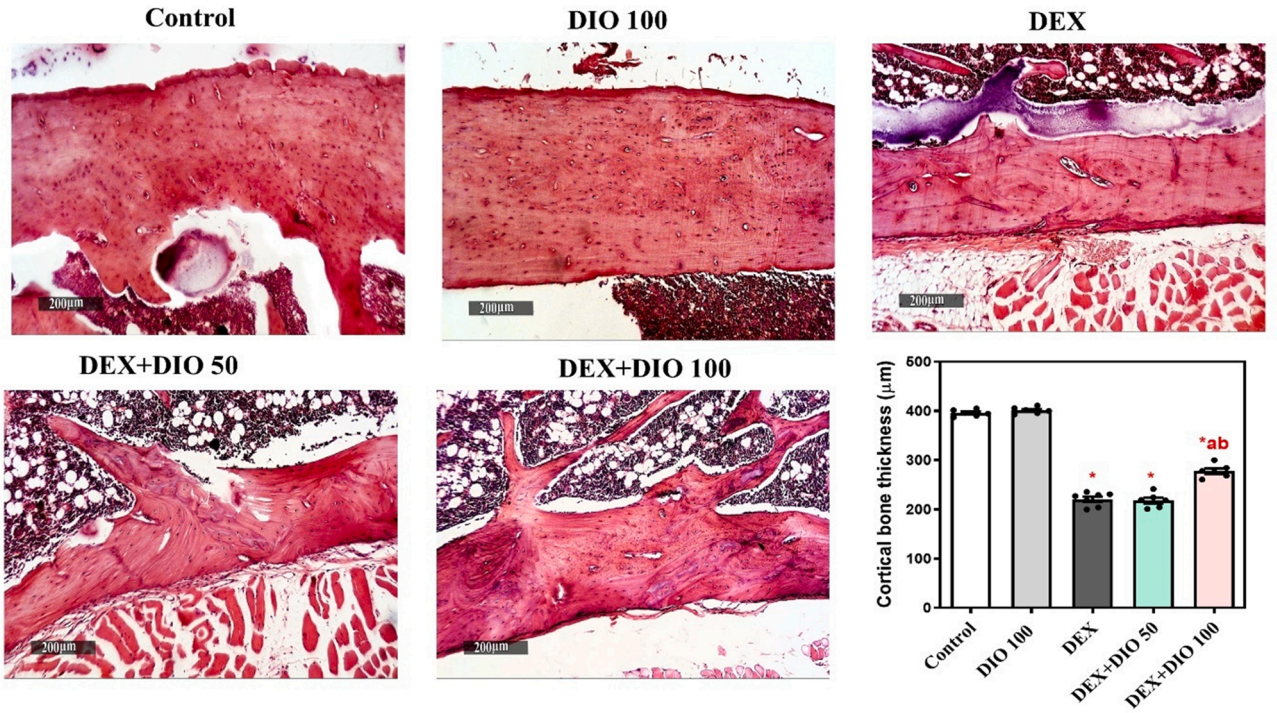

Fig. 3. Effect of diosmin on cortical bone width of DEX-induced osteoporosis in rat femur tissue. Photomicrographs of H & E-stained sections of femur cortical tissues and analysis of cortical bone width. Magnification = 100x, scale bar = 200 µm. * significant difference from control; [a] significant difference from DEX; [b] significant difference from DEX+DIO 50. DEX, dexamethasone; DIO, diosmin.

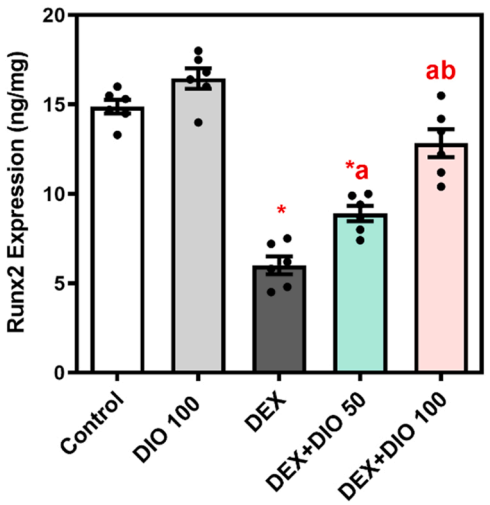

Fig. 4. Effect of diosmin on Runx2 protein expression level in femur tissue of DEX-treated rats. Runx2 protein level was measured by ELISA. Data are presented as mean ± SEM (n = 6). * significant difference from control; [a] significant difference from DEX; [b] significant difference from DEX+DIO 50. Runx2, Runt-related transcription factor-2; DEX, dexamethasone; DIO, diosmin.

3.5. Diosmin alters DEX-induced changes in RANKL and OPG mRNA expression levels

DEX group exhibited a high expression level of RANKL mRNA to more than 3-fold ($P < 0.001$) and a concomitant reduction in OPG mRNA level by 74.15 % ($P < 0.001$) in comparison to control group (Fig. 7). In turn, these changes resulted in a nearly 13-fold rise in the ratio of RANKL/OPG ($P < 0.001$) in DEX-treated rats in comparison to control group. In contrast, co-administration of DEX and diosmin significantly decreased RANKL/OPG ratio by 70.9 % and 91.6 % ($P < 0.01$ and 0.001), respectively, in comparison to DEX group (Fig. 7).

3.6. Diosmin counteracts DEX-induced bone oxidative stress

DEX administration triggered a marked decrease in the antioxidant capacity of rat femur tissue by 55.46 % for GSH and 55.17 % for SOD ($P < 0.001$) relative to control group. Additionally, there was a significant rise in the tissue content of MDA to more than 7-fold ($P < 0.001$) in comparison to control rats. On the other hand, DEX+DIO 50 and DEX+DIO 100 groups demonstrated improved production of GSH to 1.4 ($P < 0.01$) and 1.8-fold ($P < 0.001$) and SOD to 1.7 % ($P < 0.01$) and 2.3-fold ($P < 0.001$), respectively coupled with a lower level of MDA by 44.9 % and 70.4 %, respectively ($P < 0.001$) in comparison with DEX treated rats. Notably, DEX-DIO 100 group was better at counteracting DEX-induced bone oxidative stress compared to DEX-DIO 50 group ($P < 0.01$)). Of interest, exposure of rats to only diosmin (100 mg/kg) markedly increased GSH level in comparison to control group (Fig. 8).

3.7. Diosmin attenuates DEX-induced apoptosis

DEX Administration substantially induced apoptosis in femur bone tissue, as demonstrated by the elevation of the pro-apoptotic BAX protein level to about 2.7-folds as well as the decline of the anti-apoptotic BCL2 protein level by about 76.7 % in comparison to control rats ($P < 0.001$). These effects were significantly reversed in DEX+DIO 50 and DEX+DIO 100 groups. Treatment of DEX-pre-exposed rats with 50 and 100 mg/kg diosmin significantly reduced BAX by 28 % ($P < 0.01$) and 53 % ($P < 0.001$), respectively while significantly increased BCL2 to 1.7-fold ($P < 0.05$) and 2.8-fold, respectively ($P < 0.001$) compared to DEX treated rats. Interestingly, DEX+DIO 100 exerted a significant anti-apoptotic effect compared to DEX+DIO 50 group ($P < 0.01$) (Fig. 9).

4. Discussion

The current study is the first to study the influence of diosmin on the

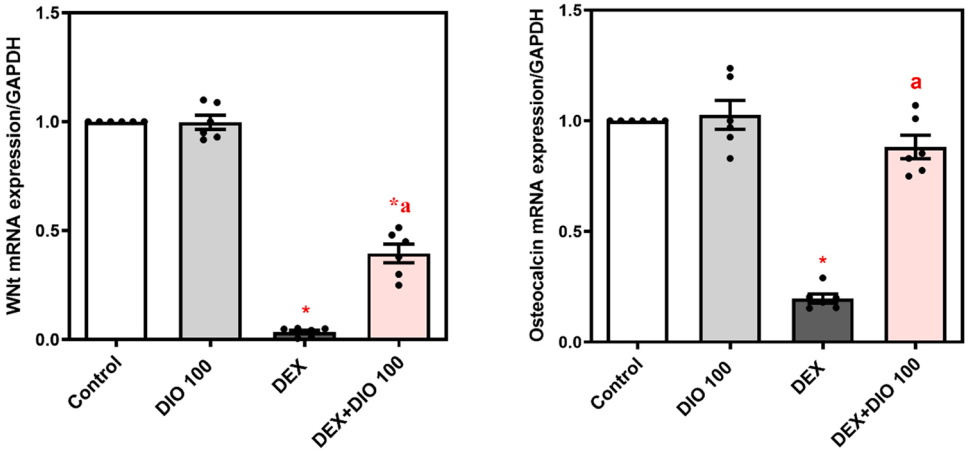

Fig. 5. Effects of diosmin on mRNA expression levels of Wnt and osteocalcin in femur tissue of DEX-treated rats. The mRNA levels were determined using qRT-PCR. Data are presented as mean ± SEM (n = 6). * significant difference from control; [a] significant difference from DEX. Wnt, Wingless; DEX, dexamethasone; DIO, diosmin.

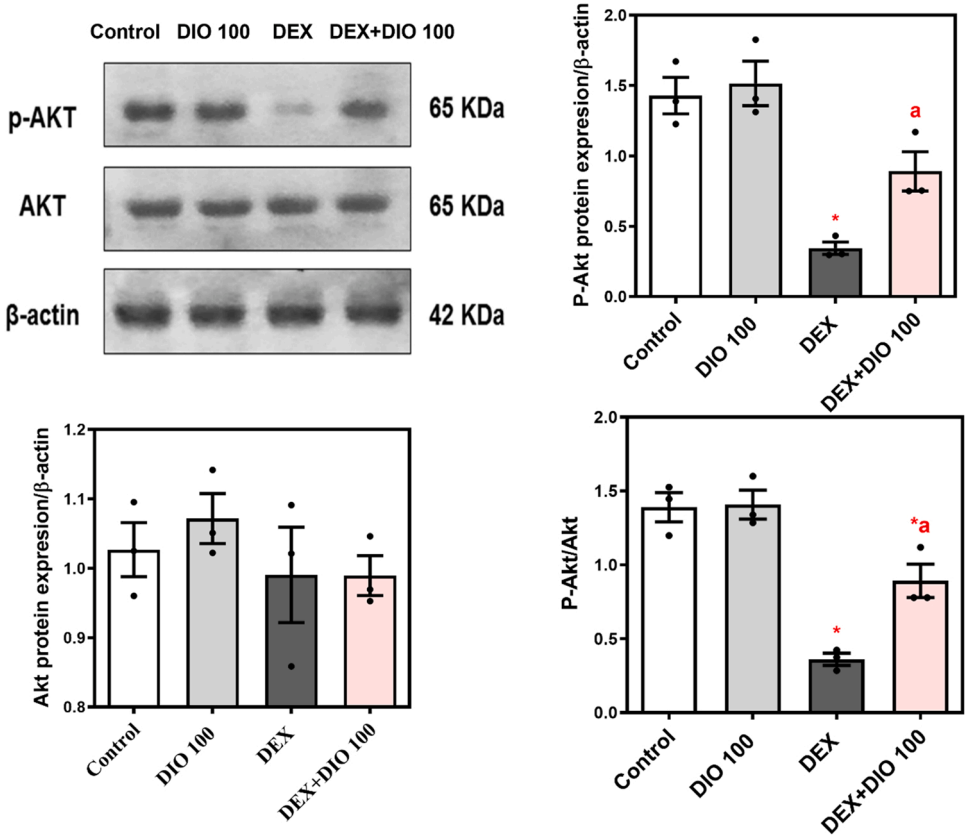

Fig. 6. Effect of diosmin on *p*-AKT protein expression level in femur tissue of DEX-treated rats. Akt and *p*-Akt protein levels were determined by western blotting. β-actin was employed as the internal loading control. Data are presented as mean ± SEM (n = 3). * significant difference from control; [a] significant difference from DEX. *p*-Akt; phosphorylated protein kinase; DEX, dexamethasone; DIO, diosmin.

bones of DEX-induced osteoporotic rats. We have found that diosmin was substantially effective at attenuating DEX-induced osteoporosis, as evidenced by maintaining the bone micro-architecture, promoting the expression of Runx2, Wnt, osteocalcin, and *p*-AKT while lowering RANKL/OPG ratio, ROS production and apoptosis. Most of these effects were significantly observed upon treatment with diosmin at 100 mg/kg relative to the lower dose of 50 mg/kg. Besides its efficacy, 100 mg/kg diosmin has proved a positive safety profile, since it didn't cause marked alterations in the parameters measured compared to normal control group.

Osteoporosis can be successfully induced in animals through pharmaceutical, surgical or dietary interventions [41]. Given the fact that prolonged administration of GCs is the most prevalent reason for iatrogenic osteoporosis [42], we chose to non-invasively induce osteoporosis in rats by using DEX. In the present study, DEX administration adversely affected the whole structure of femur bone as revealed from deteriorating the integrity of both the trabeculae, the inner bone tissue, and the cortex, the outer bone tissue. Additionally, DEX strongly

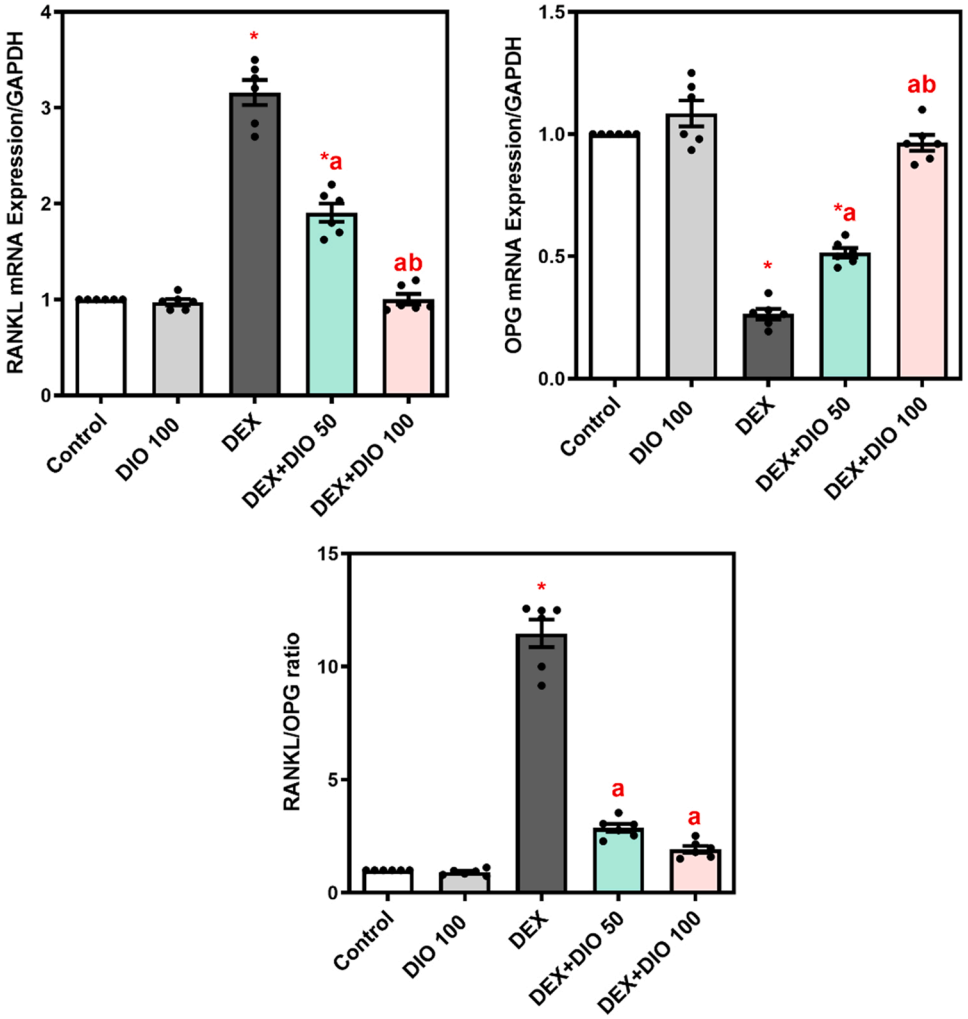

Fig. 7. Effects of diosmin on mRNA expression levels of RANKL and OPG in femur tissue of DEX-treated rats. The mRNA levels were determined using qRT-PCR. RANKL/OPG ratio was calculated by dividing RANKL mRNA expression level (% of control) by the corresponding OPG level of the same rat. Data are presented as mean ± SEM (n = 6). * significant difference from control; [a] significant difference from DEX; [b] significant difference from DEX+DIO 50. RANKL, receptor activator of nuclear factor-kB ligand; OPG, osteoprotegerin; DEX, dexamethasone; DIO, diosmin.

inhibited the mineralization of bone matrix resulting in the accumulation of osteoid, the non-mineralized bone matrix. These findings were consistent with previous studies [22,43,44]. Nevertheless, oral administration of diosmin mitigated the histo-morphometric aberrations caused by DEX, particularly the 100 mg/kg dose, indicating a positive impact of diosmin on bone health. In line, Hu et al. demonstrated that the administration of 100 mg/kg diosmin every 3 days for 3 months to ovariectomized rodents profoundly restored bone density and increased the thickness of trabecular and cortical bones [35]. Moreover, the observation that diosmin significantly decreased osteoid content might support its application for the treatment of other demineralized bone disorders, such as osteomalacia.

Further, we needed to identify the molecular determinants by which diosmin afforded protection to bone structure. The lifelong process of bone remodeling is regulated by coordination between osteoblasts and osteoclasts that is mediated by numerous signaling molecules, including Runx2, Wnt and the RANK/RANKL/OPG axis [45]. Runx2 is a crucial transcription factor involved in osteoblast differentiation [9]. Runx2-deficient mice were reported to display osteoblast dysfunction and subsequently reduced bone formation rates [46]. Moreover, many studies demonstrated that DEX caused downregulation of Runx2 mRNA and protein expression [47–50]. In agreement with this, the current study showed that Runx2 protein level was reduced in the femur bone tissues of DEX-only treated rats while restored upon concurrent treatment with diosmin. Consistent with our data, a previous study revealed that a biocomposite containing diosmin (10 or 20 μM) upregulated the mRNA and protein expression level of Runx2 in mouse mesenchymal stem cells.

Osteoblast differentiation and bone formation are not exclusively dependent on Runx2, but rather numerous signalling molecules liaise with Runx2 to regulate these processes [9]. Wnt and *p*-Akt are considered among these molecules [14,20]. Furthermore, osteocalcin is a marker of functioning, differentiated osteoblasts and bone mineralization [16]. Accordingly, our results revealed that DEX downregulated Wnt and osteocalcin mRNA expression, along with the protein expression of *p*-Akt in femur bone tissues. The obtained results are in line with earlier studies [15,21,51–53]. Furthermore, we are first to demonstrate that these effects were greatly reversed by combining DEX with diosmin. Collectively, diosmin can have the potential to promote osteoblast differentiation and subsequent bone formation.

The RANKL/RANK/OPG axis performs a key role in regulating bone remodeling, particularly bone resorption. Both RANKL and OPG are osteoblast-producing cytokines. RANKL stimulates osteoclast differentiation and bone resorption by binding its receptor on osteoclasts (i.e., pro-osteoclastic). While OPG exerts anti-osteoclastic activity by inhibiting the binding of RANKL with its receptor. Hence, the rate of bone resorption is influenced by the RANKL/PG production [45,54]. In the present study, DEX-induced osteoporotic rats exhibited upregulated RANKL mRNA expression along with downregulated OPG mRNA and consequent high RANKL/OPG ratio, indicating stimulation of bone resorption. These data are in line with previous studies [47,49,50,55]. Nevertheless, concurrent diosmin treatment along DEX ameliorated osteoclastogenesis and bone resorption, as indicated by low RANKL/OPG ratios relative to DEX only. Consistent with our findings, Shao

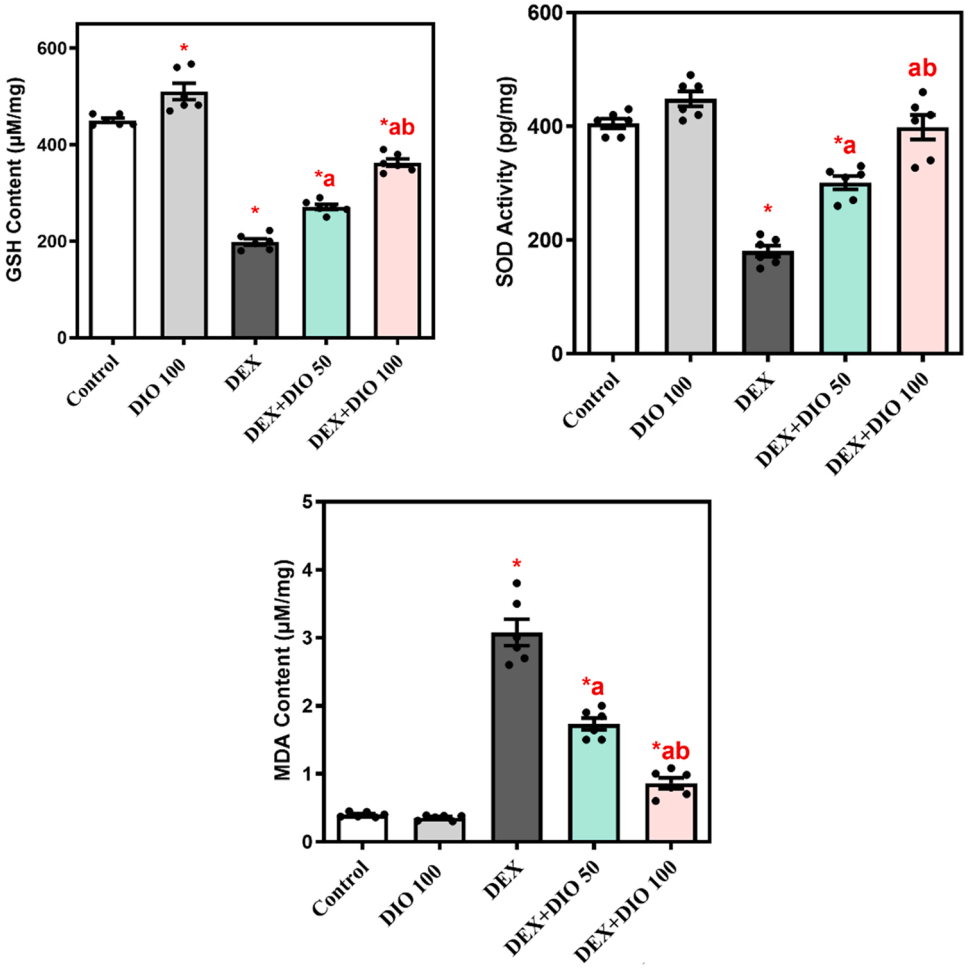

Fig. 8. Effects of diosmin on DEX-induced oxidative stress in rat femur tissue. GSH tissue content and SOD activity were measured using ELISA kits while MDA content was assessed using a colorimetric-based kit. Data are presented as mean ± SEM (n = 6). * significant difference from control; [a] significant difference from DEX; [b] significant difference from DEX+DIO 50. GSH, glutathione; SOD, superoxide dismutase; MDA, malondialdehyde; DEX, dexamethasone; DIO, diosmin.

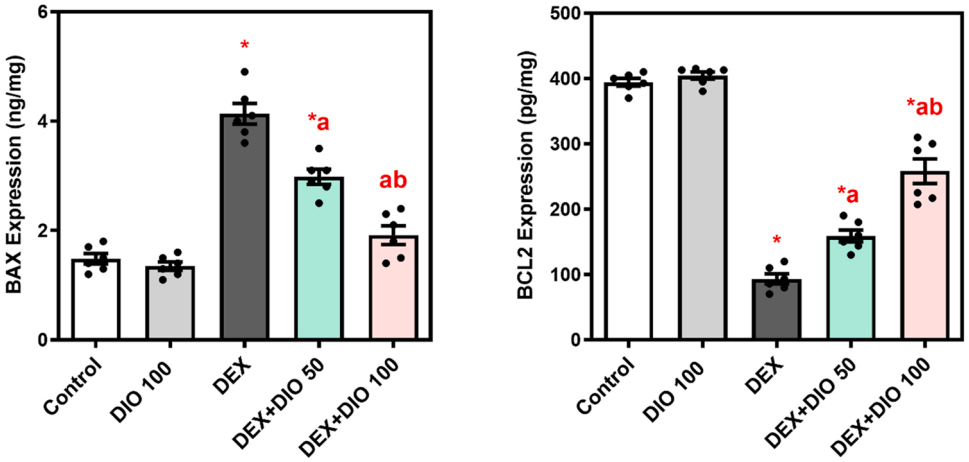

Fig. 9. Effects of diosmin on DEX-induced apoptosis in rat femur tissue. Protein expression levels of BAX and BCL2 were assessed by ELISA. Data are presented as mean ± SEM (n = 6). * significant difference from control; [a] significant difference from DEX; [b] significant difference from DEX+DIO 50. BCL2, B-cell lymphoma 2; BAX, BCL2-associated X protein; DEX, dexamethasone; DIO, diosmin.

et al. have reported that diosmin prevented RANKL-induced osteoclastogenesis in vitro [56].

Under physiologic bone resorption, osteoclasts generate ROS to help degrade bone matrix proteins, including osteocalcin [57]. These ROS can be neutralized by endogenous antioxidants, such as GSH and SOD, to interrupt bone resorption. However, excessive production of ROS can surpass the normal antioxidant defense, inducing oxidative stress and subsequently accelerated bone resorption. There is evidence that

patients with osteoporosis have a high level of oxidative markers plus a low level of antioxidants in their blood [58,59]. In the current study, administration of DEX reduced GSH content and SOD activity and increased lipid peroxidation in femur bone tissues, indicating a status of oxidative stress. These findings are in agreement with previous studies [49,50]. Diosmin is well-reported to possess antioxidant activity in vitro and in patients [60–63]. Diosmin was able to replenish the antioxidant systems that scavenged ROS generated by DEX and thereby reduced the lipid peroxidation of femur bone tissues in the study herein. To our knowledge, we are reporting for the first time the antioxidant potential of diosmin against osteoporosis.

Long-term use of GCs is associated with suppression of Runx2-induced osteoblastogenesis as well as apoptosis of already formed osteoblasts and osteocytes [42,64]. An in vivo study correlated DEX-induced apoptosis to ROS generated upon excessive use of DEX [65]. Of the crucial proteins taking part in the process of apoptosis are BAX and BCL2 which are proapoptotic and antiapoptotic proteins, respectively [66]. In the present study, administration of DEX caused apoptosis in femur bone tissues, as revealed from increased BAX and reduced BCL2 protein expression. These effects, however, were opposed upon concurrent treatment with diosmin, which is in line with previous studies reporting the anti-apoptotic property of diosmin [67,68]. These findings shed the light on the beneficial effects of diosmin toward preserving osteoblasts and osteocytes.

5. Conclusion

The findings substantiated that diosmin boosted bone formation by upregulating Runx2, Wnt, *p*-Akt, osteocalcin, OPG and BCL2, and similarly inhibited bone resorption by downregulating RANKL and ROS production. Therefore, diosmin could be a potential candidate for the management of GCs-induced osteoporosis.

Funding

The present work did not receive any specific grant from funding agencies in the public, commercial, or not-for-profit sectors.

CRediT authorship contribution statement

El-Shaimaa A. Arafa: Conceptualization, Methodology, Formal analysis, Resources, Supervision, Writing - original draft, Writing - Review & Editing, **Noran O. ELgendy**: Conceptualization, Methodology, Formal analysis, Resources, Validation, Data Curation, Writing - original draft, **Mai A. Elhemely**: Methodology, Data curation, Writing - original draft, Writing - Review & Editing, **Eglal A. Abdelaleem**: Conceptualization, Data curation, Validation, Supervision, Writing - original draft, **Wafaa R. Mohamed**: Conceptualization, Methodology, Formal analysis, Resources, Data curation, Investigation, Supervision, Writing - original draft, Writing - review & editing.

Conflict of Interest Statement

The authors declare that they have no known competing financial interests or personal relationships that could have appeared to influence the work reported in this paper.

Data availability

Data will be made available on request.

References

[1] E.M. Lewiecki, Management of osteoporosis, Clin. Mol. Allergy 2 (2004) 9.
[2] K.G. Cotts, A.S. Cifu, Treatment of osteoporosis, JAMA 319 (2018) 1040–1041.
[3] A. Catalano, G. Martino, N. Morabito, C. Scarcella, A. Gaudio, G. Basile, A. Lasco, Pain in osteoporosis: from pathophysiology to therapeutic approach, Drugs Aging 34 (2017) 755–765.
[4] M.-X. Ji, Q. Yu, Primary osteoporosis in postmenopausal women, Chronic Dis. Transl. Med. 1 (2015) 9–13.
[5] E. Stein, E. Shane, Secondary osteoporosis, Endocrinol. Metab. Clin. 32 (2003) 115–134.
[6] K. Briot, C. Roux, Glucocorticoid-induced osteoporosis, RMD Open 1 (2015), e000014.
[7] N. Guañabens, L. Gifre, P. Peris, The role of Wnt signaling and sclerostin in the pathogenesis of glucocorticoid-induced osteoporosis, Curr. Osteoporos. Rep. 12 (2014) 90–97.
[8] C.H. Peng, W.Y. Lin, K.T. Yeh, I.H. Chen, W.T. Wu, M.D. Lin, The molecular etiology and treatment of glucocorticoid-induced osteoporosis, Tzu Chi Med J. 33 (2021) 212–223.
[9] T.M. Schroeder, E.D. Jensen, J.J. Westendorf, Runx2: a master organizer of gene transcription in developing and maturing osteoblasts, Birth Defects Res C. Embryo Today 75 (2005) 213–225.
[10] G. Gu, D. Hou, G. Jiao, W. Wu, H. Zhou, H. Wang, Y. Chen, Ortho-silicic acid plays a protective role in glucocorticoid-induced osteoporosis via the Akt/Bad signal pathway in vitro and in vivo, Biol. Trace Elem. Res. (2022) 1–13.
[11] J.-y Ru, Y.-f Wang, Osteocyte apoptosis: the roles and key molecular mechanisms in resorption-related bone diseases, Cell Death Dis. 11 (2020) 1–24.
[12] M. Rossini, D. Gatti, S. Adami, Involvement of WNT/β-catenin signaling in the treatment of osteoporosis, Calcif. Tissue Int. 93 (2013) 121–132.
[13] G.J. Spencer, J.C. Utting, S.L. Etheridge, T.R. Arnett, P.G. Genever, Wnt signalling in osteoblasts regulates expression of the receptor activator of NFkappaB ligand and inhibits osteoclastogenesis in vitro, J. Cell Sci. 119 (2006) 1283–1296.
[14] T. Komori, Regulation of proliferation, differentiation and functions of osteoblasts by Runx2, Int. J. Mol. Sci. 20 (2019) 1694.
[15] N. Leclerc, T. Noh, A. Khokhar, E. Smith, B. Frenkel, Glucocorticoids inhibit osteocalcin transcription in osteoblasts by suppressing Egr2/Krox20-binding enhancer, Arthritis Rheum. 52 (2005) 929–939.
[16] A. Neve, A. Corrado, F.P. Cantatore, Osteocalcin: skeletal and extra-skeletal effects, J. Cell. Physiol. 228 (2013) 1149–1153.
[17] S.C. Moser, B.C.J. van der Eerden, Osteocalcin-A versatile bone-derived hormone, Front. Endocrinol. (Lausanne) 9 (2018) 794.
[18] L. Di Medio, M.L. Brandi, Chapter Three - Advances in bone turnover markers, in: G.S. Makowski (Ed.), Adv. Clin. Chem., Elsevier, 2021, pp. 101–140.
[19] H. Stracke, C. Schatz, H. Pralle, J. Ullmann, H. Schatz, Osteocalcin, a marker in diseases with elevated bone metabolism, Dtsch. Med. Wochenschr. 110 (1985) 1442–1446.
[20] J.-C. Xi, H.-Y. Zang, L.-X. Guo, H.-B. Xue, X.-D. Liu, Y.-B. Bai, Y.-Z. Ma, The PI3K/AKT cell signaling pathway is involved in regulation of osteoporosis, J. Recept. Signal Transduct. Res. 35 (2015) 1–6.
[21] J.-M. Pan, L.-G. Wu, J.-W. Cai, L.-T. Wu, M. Liang, Dexamethasone suppresses osteogenesis of osteoblast via the PI3K/Akt signaling pathway in vitro and in vivo, J. Recept. Signal Transduct. 39 (2019) 80–86.
[22] M. Piemontese, J. Xiong, Y. Fujiwara, J.D. Thostenson, C.A. O'Brien, Cortical bone loss caused by glucocorticoid excess requires RANKL production by osteocytes and is associated with reduced OPG expression in mice, Am. J. Physiol. -Endocrinol. Metab. 311 (2016) E587–E593.
[23] J.S. Kimball, J.P. Johnson, D.A. Carlson, Oxidative stress and osteoporosis, JBJS 103 (2021) 1451–1461.
[24] D. Barreca, G. Laganà, G. Bruno, S. Magazù, E. Bellocco, Diosmin binding to human serum albumin and its preventive action against degradation due to oxidative injuries, Biochimie 95 (2013) 2042–2049.
[25] I.J. Diel, R. Bergner, K.A. Grötz, Adverse effects of bisphosphonates: current issues, J. Support. Oncol. 5 (2007) 475–482.
[26] S.H. Gerges, S.A. Wahdan, D.A. Elsherbiny, E. El-Demerdash, Pharmacology of diosmin, a citrus flavone glycoside: an updated review, Eur. J. Drug Metab. Pharmacokinet. 47 (2022) 1–18.
[27] Z. Yun, H. Gao, P. Liu, S. Liu, T. Luo, S. Jin, Q. Xu, J. Xu, Y. Cheng, X. Deng, Comparative proteomic and metabolomic profiling of citrus fruit with enhancement of disease resistance by postharvest heat treatment, BMC Plant Biol. 13 (2013) 44.
[28] L. Silvestro, I. Tarcomnicu, C. Dulea, N.R. Attili, V. Ciuca, D. Peru, S. Rizea Savu, Confirmation of diosmetin 3-O-glucuronide as major metabolite of diosmin in humans, using micro-liquid-chromatography-mass spectrometry and ion mobility mass spectrometry, Anal. Bioanal. Chem. 405 (2013) 8295–8310.
[29] S. Bhattacharyya, S. Pal, R. Mohamed, P. Singh, S. Chattopadhyay, S.P. China, K. Porwal, S. Sanyal, J.R. Gayen, N. Chattopadhyay, A nutraceutical composition containing diosmin and hesperidin has osteogenic and anti-resorptive effects and expands the anabolic window of teriparatide, Biomed. Pharmacother. 118 (2019), 109207.
[30] T. Silambarasan, B. Raja, Diosmin, a bioflavonoid reverses alterations in blood pressure, nitric oxide, lipid peroxides and antioxidant status in DOCA-salt induced hypertensive rats, Eur. J. Pharmacol. 679 (2012) 81–89.
[31] F. Imam, N.O. Al-Harbi, M.M. Al-Harbi, M.A. Ansari, K.M. Zoheir, M. Iqbal, M. K. Anwer, A.R. Al Hoshani, S.M. Attia, S.F. Ahmad, Diosmin downregulates the expression of T cell receptors, pro-inflammatory cytokines and NF-κB activation against LPS-induced acute lung injury in mice, Pharmacol. Res. 102 (2015) 1–11.
[32] S.S. Queenthy, B. John, Diosmin exhibits anti-hyperlipidemic effects in isoproterenol induced myocardial infarcted rats, Eur. J. Pharmacol. 718 (2013) 213–218.

[33] C.C. Hsu, M.H. Lin, J.T. Cheng, M.C. Wu, Antihyperglycaemic action of diosmin, a citrus flavonoid, is induced through endogenous β-endorphin in type I-like diabetic rats, Clin. Exp. Pharm. Physiol. 44 (2017) 549–555.
[34] S. Sharma, K. Porwal, C. Kulkarni, S. Pal, S. Kumar, P. Sihota, M.C. Tiwari, R. Katekar, A. Kumar, S. Rajput, Diosmin, a citrus fruit-derived phlebotonic bioflavonoid protects rats from chronic kidney disease-induced loss of bone mass and strength without deteriorating renal function, Food Funct., (2022), pp.
[35] S. Hu, Y. Huang, Y. Chen, R. Zhou, X. Yang, Y. Zou, D. Gao, H. Huang, D. Yu, Diosmetin reduces bone loss and osteoclastogenesis by regulating the expression of TRPV1 in osteoporosis rats, Ann. Transl. Med 8 (2020) 1312.
[36] L.M.F. Lucinda, B.J.V. Aarestrup, V.M. Peters, J.E. de Paula Reis, R.S.M.F. de Oliveira, M. de Oliveira Guerra, The effect of the Ginkgo biloba extract in the expression of Bax, Bcl-2 and bone mineral content of Wistar rats with glucocorticoid-induced osteoporosis, Phytother. Res. 27 (2013) 515–520.
[37] C.F.A. Culling. Handbook of histopathological and histochemical techniques: including museum techniques, Butterworth-Heinemann, 2013.
[38] M.M. Bradford, A rapid and sensitive method for the quantitation of microgram quantities of protein utilizing the principle of protein-dye binding, Anal. Biochem. 72 (1976) 248–254.
[39] H. Towbin, T. Staehelin, J. Gordon, Electrophoretic transfer of proteins from polyacrylamide gels to nitrocellulose sheets: procedure and some applications, Proc. Natl. Acad. Sci. 76 (1979) 4350–4354.
[40] K.J. Livak, T.D. Schmittgen, Analysis of relative gene expression data using real-time quantitative PCR and the 2− ΔΔCT method, Methods 25 (2001) 402–408.
[41] T. Komori, Animal models for osteoporosis, Eur. J. Pharmacol. 759 (2015) 287–294.
[42] P. Chotiyarnwong, E.V. McCloskey, Pathogenesis of glucocorticoid-induced osteoporosis and options for treatment, Nat. Rev. Endocrinol. 16 (2020) 437–447.
[43] M.R. Elvy Suhana, H.S. Farihah, O. Faizah, A.S. Nazrun, M. Norazlina, M. Norliza, S. Ima-Nirwana, Effect of 11β-HSD1 dehydrogenase activity on bone histomorphometry of glucocorticoid-induced osteoporotic male Sprague-Dawley rats, Singap. Med. J. 52 (2011) 786–793.
[44] L. Wang, W.G. Lu, J. Shi, H.Y. Zhang, X.L. Xu, B. Gao, Q. Huang, X.J. Li, Y.Q. Hu, Q. Jie, Z.J. Luo, L. Yang, Anti-osteoporotic effects of tetramethylpyrazine via promoting osteogenic differentiation and inhibiting osteoclast formation, Mol. Med. Rep. 16 (2017) (pp).
[45] C. Soltanoff, S. Yang, W. Chen, Y.-P. Li, Signaling networks that control the lineage commitment and differentiation of bone cells, Crit. Rev. Eukaryot. gene Expr. 19 (2009) 1–46.
[46] Z. Xiao, H.A. Awad, S. Liu, J. Mahlios, S. Zhang, F. Guilak, M.S. Mayo, L.D. Quarles, Selective Runx2-II deficiency leads to low-turnover osteopenia in adult mice, Dev. Biol. 283 (2005) 345–356.
[47] Z. Yongtao, W. Kunzheng, Z. Jingjing, S. Hu, K. Jianqiang, L. Ruiyu, W. Chunsheng, Glucocorticoids activate the local renin–angiotensin system in bone: possible mechanism for glucocorticoid-induced osteoporosis, Endocrine 47 (2014) 598–608.
[48] D. Zhou, Y.X. Chen, J.H. Yin, S.C. Tao, S.C. Guo, Z.Y. Wei, Y. Feng, C.Q. Zhang, Valproic acid prevents glucocorticoid-induced osteonecrosis of the femoral head of rats, Int. J. Mol. Med. 41 (2018) 3433–3447.
[49] M.F. Tolba, A.T. El-Serafi, H.A. Omar, Caffeic acid phenethyl ester protects against glucocorticoid-induced osteoporosis in vivo: impact on oxidative stress and RANKL/OPG signals, Toxicol. Appl. Pharm. 324 (2017) 26–35.
[50] L.H. Sousa, E.V.M. Linhares, J.T. Alexandre, M.R. Lisboa, F. Furlaneto, R. Freitas, I. Ribeiro, D. Val, M. Marques, H.V. Chaves, C. Martins, G.A.C. Brito, P. Goes, Effects of atorvastatin on periodontitis of rats subjected to glucocorticoid-induced osteoporosis, J. Periodontol. 87 (2016) 1206–1216.
[51] Z. Chen, J. Xue, T. Shen, S. Mu, Q. Fu, Curcumin alleviates glucocorticoid-induced osteoporosis through the regulation of the Wnt signaling pathway, Int. J. Mol. Med 37 (2016) 329–338.
[52] A.K. Tripathi, D. Rai, P. Kothari, P. Kushwaha, K.V. Sashidhara, R. Trivedi, Benzofuran pyran hybrid prevents glucocorticoid induced osteoporosis in mice via modulation of canonical Wnt/β-catenin signaling, Apoptosis 27 (2022) 90–111.
[53] X. Ge, G. Zhou, Protective effects of naringin on glucocorticoid-induced osteoporosis through regulating the PI3K/Akt/mTOR signaling pathway, Am. J. Transl. Res 13 (2021) 6330–6341.
[54] K.A. Buckley, W.D. Fraser, Receptor activator for nuclear factor kappaB ligand and osteoprotegerin: regulators of bone physiology and immune responses/potential therapeutic agents and biochemical markers, Ann. Clin. Biochem. 39 (2002) 551–556.
[55] Y. Yang, T. Yu, H. Tang, Z. Ren, Q. Li, J. Jia, H. Chen, J. Fu, S. Ding, Q. Hao, D. Xu, L. Song, B. Sun, F. Sun, J. Pei, Ganoderma lucidum immune modulator protein rLZ-8 could prevent and reverse bone loss in glucocorticoids-induced osteoporosis rat model, Front. Pharmacol. 11 (2020) (pp).
[56] S. Shao, F. Fu, Z. Wang, F. Song, C. Li, Z.X. Wu, J. Ding, K. Li, Y. Xiao, Y. Su, X. Lin, G. Yuan, J. Zhao, Q. Liu, J. Xu, Diosmetin inhibits osteoclast formation and differentiation and prevents LPS-induced osteolysis in mice, J. Cell. Physiol. 234 (2019) 12701–12713.
[57] L.L. Key, W.C. Wolf, C.M. Gundberg, W.L. Ries, Superoxide and bone resorption, Bone 15 (1994) 431–436.
[58] H. Deveci, G. Nur, H. Çiçek, M. Karapehlivan, Evaluation of oxidative stress factors in patients with osteoporosis, Med. Sci. 6 (2017) 479–482.
[59] O.F. Sendur, Y. Turan, E. Tastaban, M. Serter, Antioxidant status in patients with osteoporosis: a controlled study, Jt. Bone Spine 76 (2009) 514–518.
[60] M.M. Abdel-Daim, H.A. Khalifa, A.I. Abushouk, M.A. Dkhil, S.A. Al-Quraishy, Diosmin attenuates methotrexate-induced hepatic, renal, and cardiac injury: a biochemical and histopathological study in mice, Oxid. Med. Cell. Longev. 2017 (2017) 3281670.
[61] M.I. Alkhalaf, Diosmin protects against acrylamide-induced toxicity in rats: roles of oxidative stress and inflammation, J. King Saud. Univ. - Sci. 32 (2020) 1510–1515.
[62] M.U. Rehman, M. Tahir, A. Quaiyoom Khan, R. Khan, A. Lateef, O.O. Hamiza, F. Ali, S. Sultana, Diosmin protects against trichloroethylene-induced renal injury in Wistar rats: plausible role of p53, Bax and caspases, Br. J. Nutr. 110 (2013) 699–710.
[63] M. Feldo, M. Woźniak, M. Wójciak-Kosior, I. Sowa, A. Kot-Waśik, J. Aszyk, J. Bogucki, T. Zubilewicz, A. Bogucka-Kocka, Influence of diosmin treatment on the level of oxidative stress markers in patients with chronic venous insufficiency, Oxid. Med. Cell. Longev. 2018 (2018) 2561705.
[64] H. Ding, T. Wang, D. Xu, B. Cha, J. Liu, Y. Li, Dexamethasone-induced apoptosis of osteocytic and osteoblastic cells is mediated by TAK1 activation, Biochem Biophys. Res Commun. 460 (2015) 157–163.
[65] W. Liu, Z. Zhao, Y. Na, C. Meng, J. Wang, R. Bai, Dexamethasone-induced production of reactive oxygen species promotes apoptosis via endoplasmic reticulum stress and autophagy in MC3T3-E1 cells, Int. J. Mol. Med. 41 (2018) 2028–2036.
[66] C.F.A. Warren, M.W. Wong-Brown, N.A. Bowden, BCL-2 family isoforms in apoptosis and cancer, Cell Death Dis. 10 (2019) 177.
[67] T.M. Ali, O.M. Abo-Salem, B.H. El Esawy, A. El Askary, The potential protective effects of diosmin on streptozotocin-induced diabetic cardiomyopathy in rats, Am. J. Med. Sci. 359 (2020) 32–41.
[68] W.Y. Liu, S.-S. Liou, T.-Y. Hong, I.-M. Liu, The benefits of the citrus flavonoid diosmin on human retinal pigment epithelial cells under high-glucose conditions, Molecules 22 (2017) 2251.